Blind Sparse Motion MRI with Linear Subpixel Interpolation

Anita Möller, Marco Maaß, Alfred Mertins

Institute for Signal Processing, University of Lübeck
moeller@isip.uni-luebeck.de

Abstract. Vital and spontaneous motion causes major artifacts in MRI. In this paper a method is presented which reduces subpixel motion artifacts via computational post processing on a complete MR scan without additional data. On the compressed sparse MRI representation, translational subpixel motion is estimated iteratively from a fully sampled, but motion corrupted k-space, and motion free images are reconstructed by linear interpolation. Motion adjusted results are presented for the Shepp-Logan phantom and brainweb data.

1 Introduction

In MRI, patient motion causes artifacts like ghost replications of the object. Therefore, spontaneous and unavoidable motion like heart beating or breathing causes problems in clinical diagnosis. Regularly applied methods such as motion avoidance through extended breath holding significantly reduces patient comfort. On the other hand, a reconstruction including motion correction is a complex task, due to the fact that each k-space point is related to two degrees of freedom in two dimensional rigid motion.

In compressed sensing, the data compressibility is used to reduce the amount of measurements that are necessary to reconstruct an image from the k-space [1]. The time needed for an MRI scan and consequently the possibility of patient motion is reduced, but it can not be excluded. Other approaches use navigators which are additionally recorded information used to calculate the motion which is included in reconstruction [2].

A sparsity based algorithm was proposed in [3]. The sparsity of MR images in the wavelet domain and the redundancy of a fully sampled k-space are used to estimate rigid motion. However, the phase-based motion model used in this approach is not suitable for realistic subpixel movement. Subpixel frequency interpolation causes ringing artifacts in the image which has to be avoided.

2 Materials and methods

The method proposed in this paper introduces a linear subpixel motion interpolation model in the image domain. The motion used for reconstruction is blindly estimated on a fully sampled k-space without additional measurements.

H. Handels et al. (Hrsg.), *Bildverarbeitung für die Medizin 2015,* Informatik aktuell,
DOI 10.1007/978-3-662-46224-9_87,

The sparsity-based estimation used in [3] is applied and extended for subpixel movement: a translational movement of the object during an MRI scan occurs as a circular shift of the object in the image domain. Let $X \in \mathbb{R}^{m,n}$ be an arbitrary discrete image. A circular shift in one image dimension by $b = n + d$, $n \in \mathbb{N}$, $d \in (0, 1]$ with linear interpolation between adjacent pixels can be formulated using convolution matrices of the form

$$C_d = \begin{bmatrix} 1-d & d & 0 & 0 & \cdots & 0 \\ 0 & 1-d & d & 0 & \cdots & 0 \\ \vdots & \ddots & \ddots & \ddots & \ddots & \vdots \\ 0 & \cdots & 0 & 1-d & d & 0 \\ 0 & \cdots & \cdots & 0 & 1-d & d \\ d & 0 & \cdots & \cdots & 0 & 1-d \end{bmatrix} \tag{1}$$

A two dimensional positive image shift $S_b[X]$ with $b = (b^y, b^x)$ is calculated as

$$S_b[X] = C_{d^y} C_1^{n^y} X \left(C_1^{n^x}\right)^T C_{d^x}^T \tag{2}$$

where $n^x, n^y \in \mathbb{N}$ denote the numbers of full pixel shifts in both directions and d^x, d^y denote subpixel shifts (upper indices x, y denote directions). Due to circularity, negative shifts are realized as large positive shifts.

2.1 Recording of k-space

In MR imaging, the k-space $K \in \mathbb{R}^{m,n}$ is recorded. More exactly, one line of the k-space denoted by $K(k^y, \cdot)$, $k^y = 1, ..., m$ is generated at one measurement read-out. Assuming that the movement during one measurement is constant due to short recording time, one line of the recorded k-space $\hat{K}$ gained from a shifted image $S_{b_{k^y}}[X]$ can be modeled as

$$\hat{K}(k^y, \cdot) = \boldsymbol{e}_{k^y}^T \mathcal{F}^y S_{b_{k^y}}[X] \mathcal{F}^x \tag{3}$$

by applying the Fourier transform matrices $\mathcal{F}^y, \mathcal{F}^x$ in x- and y-direction, respectively and selecting one line with the unit vector $\boldsymbol{e}_{k^y}$. Let $F[X]$ be an operator which applies the Fourier transform to X in the way $F[X] = \mathcal{F}^y X \mathcal{F}^x$. Then, the whole k-Space is gained as

$$\hat{K} = F_B[X] = \left[e_{k^y}^T F\left[S_{b_{k^y}}[X]\right]\right]_{k^y=1}^m \quad \text{with} \quad B = [b_{k^y}^y, b_{k^y}^x]_{k^y=1}^m \tag{4}$$

A further reformulation step uses the property that the multiplication of two convolution matrices stays a convolution matrix. Also, $\mathcal{F}C = D\mathcal{F}$, $C^T\mathcal{F} = \mathcal{F}D$ holds for a convolution matrix C and a corresponding $D = \mathcal{F}C\mathcal{F}^H$ with $\mathcal{F}$ being a one-dimensional Fourier matrix and D a diagonal matrix. Now, (4) yields

$$\hat{K} = F_B[X] = \left[e_{k^y}^T D_{k^y}[F[X]]\right]_{k^y=1}^m =: Q_B[F[X]] \tag{5}$$

2.2 Reconstruction algorithm

It is assumed that an MR image without motion artifacts has the highest sparsity compared to images gained from the same but moved object [3]. This assumption is founded in MRI artifacts being shifted ghost replications of the object. Using the wavelet transform as sparsifying transform, the problem is formulated similar to [4] as

$$\arg\min_{X,B} \left\| \hat{K} - Q_B\left[F\left[X\right]\right] \right\|_F \text{ subject to } \left\|\mathcal{W}X\right\|_1 \leq c,\ B \in \mathcal{D}_B \tag{6}$$

The sparsifying constant $c > 0$ has to be determined experimently in the later given algorithm with a few propositions [4]. The space $\mathcal{D}_B$ defines motion constraints. For each point in one k-space line, the same translational motion should be estimated and also subpixel motion is permitted as advantage to [3].

The iterative motion estimation is divided into three steps [3]. At first, a sparse representation $\tilde{X}$ of $\hat{X} = F^{-1}[\hat{K}]$ is found. Secondly, the motion between $\tilde{X}$ and $\hat{X}$ is calculated. At the third step, the estimated motion is used to find a better $\tilde{K}$ as approximation of $\hat{K}$ to reconstruct the corresponding new $\tilde{X}$ with which the algorithm is started again.

3 Results

The presented algorithm was tested on the Shepp-Logan phantom and human brain images [5]. As different sizes of the images were tested with similar results, representatives of 256×256 pixels for the Shepp-Logan phantom and of 217×181 pixels for the brain images were chosen (Fig. 1).

Starting from the assumptions $\tilde{B} = 0$ and $\tilde{K} = \hat{K}$, the subproblem

$$\tilde{X} = \arg\min_{X} \left\| \tilde{K} - Q_{\tilde{B}}\left[F\left[X\right]\right] \right\|_F \text{ subject to } \left\|\mathcal{W}X\right\|_1 \leq c \tag{7}$$

is solved by an algorithm proposed in [3], which keeps the largest entries in $\mathcal{W}F^{-1}\left[\tilde{K}\right]$, so that $\left\|\mathcal{W}F^{-1}\left[\tilde{K}\right]\right\|_1 \leq c$, and sets all other entries to zero ($\mathcal{W}$ denotes the wavelet transform). This step solves the subproblem

$$\tilde{B} = \arg\min_{B} \left\| \tilde{K} - Q_B\left[F\left[\tilde{X}\right]\right] \right\|_F \text{ subject to } B \in \mathcal{D}_B \tag{8}$$

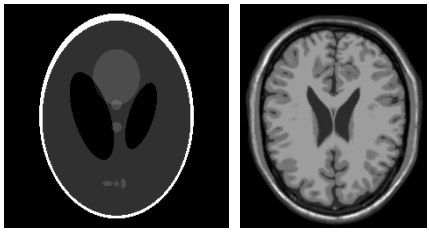

Fig. 1. Shepp-Logan phantom (left) and human brain image (right).

As the properties of the Fourier transform deliver, the relation of the k-space $K \in \mathbb{R}^{m,n}$ of an unmoved object and $\hat{K}$ is found in the phase and written as

$$\hat{K}\left(k^y, k^x\right) = \exp\left(-i2\pi\left(\frac{k^y}{m} b_{y_{k^y}} + \frac{k^x}{n} b_{x_{k^y}}\right)\right) K\left(k^y, k^x\right) \tag{9}$$

as explained in [4]. This property is used for motion estimation based on [2]. For each k-space line, the motion is calculated separately between $\mathcal{F}\tilde{X}$ as motion corrected k-space approximation and $\tilde{K}$. As derived in [2], the motion in x-direction by $b^x_{k^y}$ can be calculated as index of the maximal cross-correlation of $\mathcal{F}\tilde{X}(k^y, \cdot)$ and $\tilde{K}(k^y, \cdot)$. To extend this for subpixel motion, a parabola is generated with the correlation maximum and its both neighbors. The index of the parabola maximum approximates the shift $b^x_{k_y}$. The shift $b^y_{k_y}$ is calculated from the phase of the maximal correlation [2].

To update $\tilde{K}$ with the estimated $\tilde{B}$ in order to find a better approximation for the motion free k-space, the shift operation has to be revoked. Starting with the shifts b^x in x-direction and (3), the following recursion is derived

$$\hat{K}\left(k^y, \cdot\right) = e_{k^y} \mathcal{F}^y \hat{X} \mathcal{F}^x \tag{10}$$

$$\Leftrightarrow \quad \hat{K}\left(k^y, \cdot \mathcal{F}^{x^{-1}}\right) = e_{k^y} \mathcal{F}^y C_{d^y} C_1^{n^y} X (C_1^{n^x})^T C_{d^x}^T \tag{11}$$

$$\Leftrightarrow \underbrace{\hat{K}\left(k^y, \cdot\right) \mathcal{F}^{x^{-1}} C^T_{-d^x+1} \left(C_0^{n^x+1}\right)^T}_{\hat{K}_y} = e_{k^y} \mathcal{F}^y C_{d^y} C_1^{n^y} X \tag{12}$$

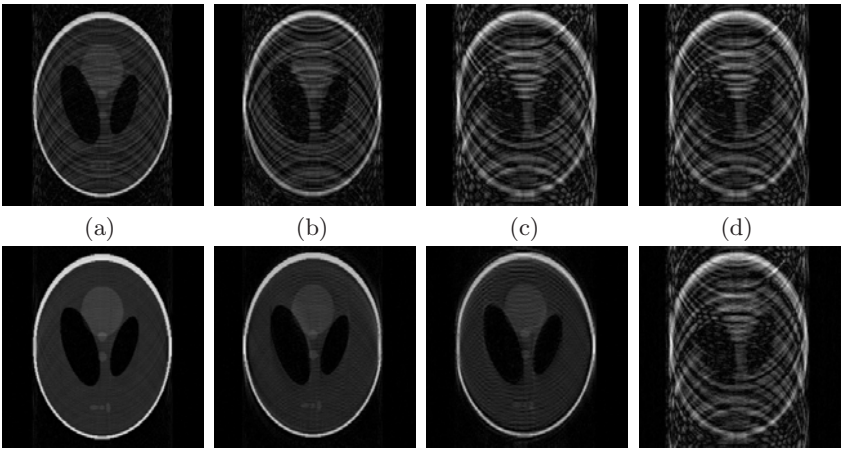

Fig. 2. Moved Shepp-Logan phantom with maximal motion of (a): 2, (b): 5, (c),(d): 8 pixels in all k-space lines. Related reconstructed images gained by the presented algorithm (e)-(g) and gained by reconstruction algorithm from [3] (h).

Applying $\tilde{b}^x$ with (12) to the current approximation $\tilde{K}$ delivers an estimate $\tilde{K}_y$ that is motion free in x-direction. With (9) follows

$$\hat{K}_y\left(k^y,\cdot\right) = \exp\left(-i2\pi\frac{k^y}{m}b^y_{k^y}\right)K_y\left(k^y,\cdot\right) \tag{13}$$

and the recursion is given by

$$\exp\left(i2\pi\frac{k^y}{m}b^y_{k^y}\right)\hat{K}_y\left(k^y,\cdot\right) = K_y\left(k^y,\cdot\right) \tag{14}$$

The full k-space is $K = \mathcal{F}\mathcal{F}^{y^{-1}}K_y$. Applying $\tilde{b}^y$ in this way to $\tilde{K}_y$ results in a new estimation for $\tilde{K}$, which is used as starting point for the next iteration.

The algorithm stops if no significant motion higher than a threshold (here selected as 0.1 pixels) is estimated anymore.

As the repeated application of the convolution matrix in the x-directional reconstruction could constitute a low pass filtering a global motion variable $G \in \mathbb{R}^{m,2}$ is defined to avoid blurring. It starts at $G = 0$ and $\tilde{B}$ is added in each iteration. The final estimation $\tilde{K}$ is generated by applying G in an extra reconstruction step to $\hat{K}$ at the algorithm end.

Randomly chosen k-space lines were calculated directly from moved images of the object. The motion was simulated in the image domain by a circularly shift of up to 8 pixels independently in both directions. This simulation is similar to the random k-space line recording order in MRI. In some simulations, only half

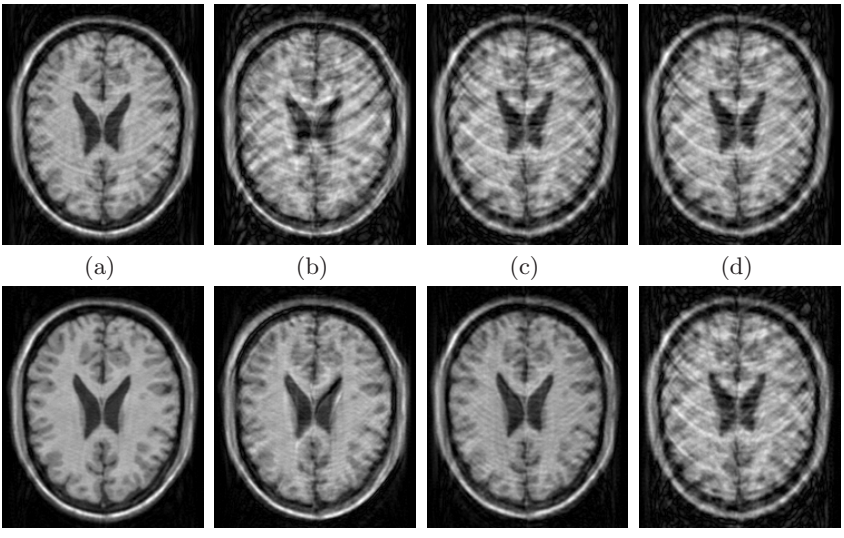

Fig. 3. Moved brain image with maximal motion of (a): 2, (b)-(d): 5 pixels in all ((a),(c),(d)), half (b) of the k-space lines. Related reconstructed images gained by the presented algorithm (e)-(g) and gained by reconstruction algorithm from [3] (h).

of the k-space lines were chosen randomly and calculated from shifted images, the remaining ones were calculated from the original. The images gained from the inverse Fourier transform of so produced k-spaces are shown in the upper lines of Figs. 2 and 3.

The sparsifying step was tested with different wavelets (Daubechies and Symlets), and due to its good results, the Haar wavelet was selected. For the calculation of the sparsifying constant, a variable $a \in \mathbb{R}^+$ was chosen with $c = a \left\| \mathcal{W} X \right\|_1$. For the test environment, $a \in [0.4, 0.6]$ turned out to be suitable.

The results gained by reconstruction with the proposed blind motion compensation are shown in Fig. 2 (e)-(g), 3 (e)-(g). Even for large motion shifts, an excellent reconstruction of image details is achieved. Image structures that were not even noticeable before get revealed. Only a small amount of noise remains. As reference, reconstruction results gained by [3] are shown in 2 (h), 3 (h). With under 30 seconds, the enhanced algorithm is much faster than [3] on a similar computer. In addition to motion interpolation via convolution matrices, the approach was tested for a cubic translational motion interpolation in the image domain, for which the same quality of results was achieved.

4 Discussion

The proposed approach offers a promising and fast MRI motion correction with subpixel accuracy without collecting additional data. MRI reconstruction gets more stable. For a clinician, a diagnostic of in distorted images not noticeable structures gets possible. In future works, the aim is to extend the algorithm to more general non-rigid motion. New methods for motion estimation need to be tested, and an adaption rule for the sparsifying constant has to be found. A noise reduction step could be inserted to erase remaining small artifacts.

References

1. Lustig M, Donoho DL, Santos JM, et al. Compressed sensing MRI. IEEE Signal Process Mag. 2008;25:72–82.
2. Lin W, Huang F, Börnert P, et al. Motion correction using an enhanced floating navigator and GRAPPA operations. Magn Reson Med. 2009;63:339–48.
3. Yang Z, Zhang C, Xie L. Sparse MRI for motion correction. Proc IEEE Int Symp Biomed Imaging. 2013; p. 962–5.
4. Yang Z. Analysis, Algorihms and Applications of Compressed Sensing. Nanyang Technological University. Singapore; 2013.
5. Cocosco CA, Kollokian V, Kwan RKS, et al. BrainWeb: online interface to a 3D MRI simulated brain database. NeuroImage. 1997;5(4):425.